# Androgens differentially modulate glucocorticoid effects on adipose tissue and lean mass

Sommers, V.; David, K.; Helsen, C.; Moermans, K.; Stockmans, I.; Ferrari, G.; ... ; Dubois, V.

Society for Endocrinology

*Journal of Endocrinology* (2025) **264** e240061
https://doi.org/10.1530/JOE-24-0061

Received 22 February 2024
Accepted 20 January 2025
Available online 20 January 2025
Version of Record published 31 January 2025

RESEARCH

# Androgens differentially modulate glucocorticoid effects on adipose tissue and lean mass

Vera Sommers[1,2,3], Karel David[4,5], Christine Helsen[1], Karen Moermans[4], Ingrid Stockmans[4], Gabriele Ferrari[6], Ruslan I Dmitriev[6], Steve Stegen[4], Onno C Meijer[2,3,*], Jan Kroon[2,3,*], Frank Claessens[1,*] and Vanessa Dubois[1,7,*]

[1]Laboratory of Molecular Endocrinology, Department of Cellular and Molecular Medicine, KU Leuven, Leuven, Belgium
[2]Department of Internal Medicine, Division of Endocrinology, Leiden University Medical Center, Leiden, Netherlands
[3]Einthoven Laboratory for Experimental Vascular Medicine, Leiden University Medical Center, Leiden, Netherlands
[4]Laboratory of Clinical and Experimental Endocrinology, Department of Chronic Diseases and Metabolism, KU Leuven, Leuven, Belgium
[5]Department of Endocrinology, University Hospitals Leuven, Leuven, Belgium
[6]Tissue Engineering and Biomaterials Group, Department of Human Structure and Repair, Faculty of Medicine and Health Sciences, Ghent University, Ghent, Belgium
[7]Laboratory of Basic and Translational Endocrinology, Department of Basic and Applied Medical Sciences, Faculty of Medicine and Health Sciences, Ghent University, Ghent, Belgium

Correspondence should be addressed to V Dubois: vanessa.dubois@ugent.be

*(O C Meijer, J Kroon, F Claessens and V Dubois contributed equally to this work)

## Abstract

Glucocorticoids and androgens affect each other in several ways. In metabolic organs, such as adipose tissue and the liver, androgens enhance glucocorticoid-induced insulin resistance and promote fat accumulation in male mice. However, the direct contribution of the androgen receptor (AR) to these effects is unknown. Furthermore, it is unclear whether the potentiating effect of androgens on glucocorticoid signaling in fat extends to other tissues, such as skeletal muscle and bone. In this study, we used two complementary models for androgen deprivation (orchidectomy and chemical castration) to investigate the effects of dihydrotestosterone (DHT) on corticosterone (CORT). We found that after 2 weeks of intervention, DHT alone did not affect fat mass but increased lean mass, while CORT increased fat mass and decreased lean mass. Co-supplementation with DHT counteracted the CORT effect on lean mass but enhanced its effect on adiposity. Glucocorticoid induction of *Gilz*, *Fkbp5* and *Mt2a* in gonadal white adipose tissue depended on the presence of androgens, while in interscapular brown adipose tissue, these genes responded to glucocorticoids also without androgens. To directly assess the impact of the AR on the glucocorticoid response, male global AR knock-out mice were exposed to CORT and compared to WT littermates. CORT exposure resulted in an increase in fat mass and a decrease in lean mass in both genotypes. In conclusion, functional AR signaling is dispensable for the metabolic response to glucocorticoids. However, androgen signaling in WT mice modulates glucocorticoid response in a tissue-dependent manner, by counteracting lean mass and potentiating fat mass effects.

Keywords: androgens; glucocorticoids; adipose tissue; muscle

## Introduction

Glucocorticoids are steroid hormones synthesized by the adrenal glands in a circadian manner and in response to stress. Glucocorticoids exert various physiological functions, including the regulation of adipose tissue metabolism, muscle energy balance and bone homeostasis (Kadmiel & Cidlowski 2013). Patients with hypercortisolism, whether in Cushing's syndrome or due to other causes, exhibit increased adiposity, dyslipidemia,

Published by Bioscientifica Ltd.
https://joe.bioscientifica.com

muscle wasting and osteoporosis (Poetker & Reh 2010, Huan *et al.* 2014). The consequences of excess glucocorticoid exposure are also observed in patients using synthetic glucocorticoids. Synthetic glucocorticoids are extensively used in clinical practice to treat acute and chronic inflammatory diseases (Poetker & Reh 2010, Hua *et al.* 2020), but treatment is frequently accompanied by adverse effects reminiscent of those seen in Cushing's syndrome. Hence, a better understanding of the mechanisms underlying glucocorticoid effects on metabolic tissues is crucial to improve their use in clinical practice.

Glucocorticoids exert most of their actions through binding to the glucocorticoid receptor (GR), a ligand-activated transcription factor belonging to the nuclear receptor family. Besides ligand availability, GR transcriptional activity is influenced by several factors, including receptor levels and interaction with other transcriptional regulators (Vandevyver *et al.* 2014, De Bosscher *et al.* 2020, Præstholm *et al.* 2020). Furthermore, glucocorticoid action is balanced via intracellular enzymatic (in)activation. 11-beta-hydroxysteroid dehydrogenase type 1 (11β-HSD1) converts inactive glucocorticoids into the active form (Walker & Andrew 2006), while 11-beta-hydroxysteroid dehydrogenase type 2 (11β-HSD2) catalyzes the reverse reaction and inactivates glucocorticoids (Coutinho *et al.* 2012). Glucocorticoid action is often sexually dimorphic, in particular in metabolic organs such as adipose tissue and liver (Duma *et al.* 2010, Quinn *et al.* 2014, Gasparini *et al.* 2019, Kaikaew *et al.* 2019). Interestingly, observations in patients with acute and chronic inflammatory diseases revealed sex differences in the response to glucocorticoid treatment, with women being more sensitive to the metabolic-syndrome-like symptoms and men being more sensitive to osteoporosis (Pecori Giraldi *et al.* 2003, Valassi *et al.* 2011, Savas *et al.* 2017, Kroon *et al.* 2020). Altogether, these findings point toward a possible crosstalk between glucocorticoids and sex hormones.

The interplay between glucocorticoids and androgens has been investigated in prostate cancer, with various studies reporting substitution of the androgen receptor (AR) by the GR on the chromatin of anti-androgen-resistant prostate cancer cells (Davies & Rushmere 1990, Arora *et al.* 2013, Sahu *et al.* 2013, Paakinaho & Palvimo 2021). In metabolic tissues, we previously showed that the AR antagonist enzalutamide modulates glucocorticoid action in adipose tissue and liver (Spaanderman *et al.* 2018, Buurstede *et al.* 2022). Seibel and colleagues demonstrated that endogenous androgens exacerbate glucocorticoid-induced insulin resistance and fat accumulation in male mice (Gasparini *et al.* 2019). Whether this sensitizing effect of androgens holds true for glucocorticoid action on other tissues, such as skeletal muscle and bone, remains to be determined. Furthermore, the direct contribution of the AR to this effect is unknown.

In this study, we explored the impact of androgen status on the metabolic response to glucocorticoids in multiple organs by using two different mouse models of endogenous androgen deprivation. First, surgical castration by orchidectomy (ORX) was applied. Second, we used chemical castration by treatment with the gonadotropin-releasing hormone (GnRH) antagonist degarelix (DGX) (Kim *et al.* 2021*b*) to validate the findings of the ORX model. In both models, we compared the effects of corticosterone (CORT), the main glucocorticoid in rodents, alone or in combination with the non-aromatizable androgen dihydrotestosterone (DHT). To examine the direct contribution of the AR to the effects of glucocorticoids, CORT action was assessed in a global androgen receptor knock-out (ARKO) mouse model and a comparison was made with wild-type (WT) littermates (De Gendt *et al.* 2004).

## Materials and methods

### Animal care

Mice were group-housed (3–4 mice/cage) at a constant temperature of 20°C with a 12 h light:12 h darkness cycle and had access to water and standard chow *ad libitum*. The animal experiments were conducted following the KU Leuven guidelines for animal experimentation and approved by the KU Leuven ethical committee (P190/2020).

### Experimental design

To study the effect of androgen signaling on the metabolic response to glucocorticoids, 14-week-old male WT mice (C57BL/6J background) (Charles River, USA) were either surgically castrated via ORX or chemically castrated using the GnRH antagonist DGX as detailed in the 'Castration procedure and hormone administration' section below. At the moment of castration, mice were supplemented with vehicle (VEH), DHT, CORT or a combination of both (CORT + DHT) for 2 weeks. Control mice (SHAM) received either a sham surgery (to control for ORX) or a subcutaneous injection with aqua ad iniectabilia (to control for DGX) and were supplemented with VEH (details in the 'Castration procedure and hormone administration' section below). To study the role of the AR in the glucocorticoid response, 14-week-old male ARKO mice and WT littermates (C57BL/6J background) (De Gendt *et al.* 2004) received either VEH or CORT for 2 weeks (details in the 'Castration and hormone administration' section below). Phenotypical characterization and tissue collection were performed as follows: on day 0 (baseline), day 7 (intermediate time point) and day 14 (end point) of the intervention, body weight was assessed and body composition was determined using echoMRI. On day 11, mice were

*Journal of Endocrinology* (2025) **264** e240061
https://doi.org/10.1530/JOE-24-0061

fasted for 6 h and blood was collected via a tail bleed to measure fasting blood glucose and insulin levels in serum. All mice were euthanized at day 14 (at random between 08:00 and 16:00 h to avoid circadian rhythm differences between the experimental groups), i.e., at 16 weeks of age, by $CO_2$ asphyxiation followed by cardiac puncture. Wet weights of androgen- and glucocorticoid-sensitive organs, fat pads and gastrocnemius muscle were determined. Body weight (lean/fat mass) was affected by the hormonal manipulations, and for this reason, we reported absolute organ weights rather than corrected for body weight. Femora were kept in PBS at −20°C until biomechanical testing. Tibiae were fixed overnight in 2% paraformaldehyde and stored in PBS at 4°C until microCT and histological analysis.

## Castration procedure and hormone administration

Surgical castration by ORX was performed under isoflurane anesthesia (3% for induction; 2% for maintenance). Shortly, an incision was made in the abdomen, the testes were removed, and the incision was sutured. The SHAM mice underwent the same procedure, except for removing the testes. Chemical castration using the GnRH antagonist DGX was performed under isoflurane anesthesia. Mice were subcutaneously injected with 25 mg/kg DGX (Ferring Pharmaceuticals, Switzerland) dissolved in aqua ad iniectabilia. SHAM mice received a subcutaneous injection with aqua ad iniectabilia. After castration and/or hormone administration, all animals received analgesia with meloxicam (Metacam, Boehringer Ingelheim, Germany). At the moment of castration, mice were subcutaneously implanted with a silastic stick and a pellet in the dorsal region. VEH-administered mice received an empty 1.5 cm silastic stick (Silclear Tubing; Degania Silicone, Germany) (VEH stick) and a pellet containing 100 mg cholesterol (Sigma-Aldrich, USA) (VEH pellet). DHT-administered mice received a 1.5 cm silastic stick filled with DHT (Fluka) (DHT stick; daily release of 75 μg DHT/day (Vandenput *et al.* 2002)) and a VEH pellet. CORT-administered mice received a VEH stick and a pellet (CORT pellet) containing 12.5 mg CORT (Sigma-Aldrich) and 87.5 mg cholesterol (Sigma-Aldrich) (Koorneef *et al.* 2020). CORT + DHT animals received both a DHT stick and a CORT pellet. SHAM mice received a VEH stick and a VEH pellet.

## EchoMRI

Total body fat mass and lean body mass were determined by quantitative magnetic resonance (EchoMRI-100H Analyzer, Echo Medical Systems, USA) according to the manufacturer's instructions.

## Serum measurements

Mice were individually housed for 6 h (between 08:00 and 14:00 h) without access to food. Subsequently, blood was collected via tail cut, and fasting glucose levels were measured with an Accu-Chek glucometer (Roche, Germany). Fasting insulin levels were determined with the Ultra Sensitive Mouse Insulin ELISA Kit (Crystal Chem, USA) according to the manufacturer's instructions. As an indirect readout of insulin sensitivity, the homeostasis model assessment of insulin resistance (HOMA-IR) was used: HOMA-IR = fasting glucose (mg/dL) × fasting insulin (μU/mL)/405 (Okita *et al.* 2013). Serum collected at sacrifice was used to measure procollagen type 1 N-terminal propeptide (P1NP), a marker of bone formation, and tartrate-resistant acid phosphatase type 5b (TRAcP 5b), a marker of bone resorption. P1NP levels were measured with the Rat/Mouse PINP EIA kit (Immunodiagnostic Systems, UK) and TRAcP 5b levels were measured with the Mouse TRAP ELISA kit (Immunodiagnostic Systems) according to the manufacturer's instructions.

## Micro-computed tomography (microCT)

Tibiae were scanned using the Bruker SkyScan 1272 (Bruker, Belgium) with 5 μm pixel size, 0.5 mm Al filter, 60 kV, 83 μA, 180° angular rotation at 0.4° steps and 3,000 ms integration time. Images were reconstructed using the reconstruction software NRecon (Bruker), and morphometric parameters were calculated using CTAn (Bruker) as previously described (Kim *et al.* 2020). For trabecular bone, a 0.5 mm segment was analyzed starting at 0.75 mm from the proximal growth plate and moving toward the diaphysis. For cortical bone, a 0.5 mm region of interest was selected starting at 3 mm from the proximal growth plate and moving toward the diaphysis.

Parameters are reported according to the American Society for Bone and Mineral Research (ASBMR) guidelines (Whittier *et al.* 2020) and include trabecular bone volume fraction (BV/TV, %), trabecular number (Tb. N, 1/mm), trabecular thickness (Tb. Th, mm), trabecular separation (Tb. Sp, mm), cortical thickness (Ct. Th, mm), total tissue area (T. Ar, $mm^2$), cortical area (Ct. Ar, $mm^2$), medullary area (Ma. Ar, $mm^2$), endocortical perimeter (Ec.Pm, mm), periosteal perimeter (Ps. Pm, mm), cortical porosity (%) and polar moment of inertia (MMI, $mm^4$).

## Biomechanical testing

Femora collected at sacrifice were kept in PBS at −20°C. After complete thawing, samples were kept hydrated and a destructive three-point bending test was performed using the LRXplus universal testing machine (Lloyd Instruments, USA) with a 100 N load cell. The diameter of the femora was measured with a caliper at the mid-diaphysis immediately prior to the test. The femora were positioned on two

supporting pins with a 6 mm span, and the loading point was positioned on the mid-diaphysis of the femur. The loading pin was gradually moved downward at a speed of 0.1 mm/s. The test was stopped at the breaking point, i.e., when the femur fractured. The load–displacement curve was used to calculate ultimate bone strength.

### RNA extraction and real-time quantitative PCR

Fat pads and gastrocnemius muscle collected at sacrifice were snap-frozen in liquid nitrogen and stored at −80°C until further processing. Total RNA was extracted using TRIzol reagent (Invitrogen, USA) according to the manufacturer's instructions for gastrocnemius muscle. A slight modification was made for RNA extraction from the fat pads, i.e., 1 mL TRIzol reagent was added, followed by the addition of 50 μL Tween-20 per sample. DNA was synthesized from 1 μg RNA using the FastGene Scriptase Ready kit (NIPPON Genetics Europe, Germany). The real-time quantitative PCR (RT-qPCR) was performed using Fast SYBR Green Master Mix and the StepOnePlus Real-Time PCR system (Applied Biosystems, USA). Gene expression was normalized to the expression of the *Hprt* housekeeping gene for fat pads and *18S* for gastrocnemius and expressed relative to the control group ($2^{-\Delta\Delta Ct}$ method). Primer sequences are described in Supplementary Table S1 (see section on Supplementary materials given at the end of the article). All primers were designed to hybridize to different exons, and generation of single correct amplicons was checked by melting curve analysis.

### Histology of adipose and bone tissue

Gonadal white adipose tissue (gWAT) samples collected at sacrifice were fixed in 4% paraformaldehyde overnight and embedded in paraffin. Adipose tissue sections (5 μm) were stained with hematoxylin and eosin (H&E). Images were taken on a Zeiss Axioscan 7. Adipocyte size was determined in seven representative fields per section using the Adiposoft plugin of the ImageJ software (version 1.53q).

Tibiae collected at sacrifice were fixed overnight in 2% paraformaldehyde and decalcified in 0.5 M EDTA in PBS (pH 7.4) for 2 weeks at 4°C. Decalcified bones were dehydrated in graded ethanol concentrations and embedded in paraffin. Bone sections (4 μm) were stained with H&E to visualize osteoblasts, and tartrate-resistant acid phosphatase staining was used to visualize osteoclasts (Stegen *et al.* 2024). Osteoblast- and osteoclast-related parameters were quantified on at least two sections within defined regions of interest, starting at 150 μm below the growth plate. All data are calculated and shown according to the ASBMR standardized histomorphometry nomenclature (Dempster *et al.* 2013).

### Statistical analysis

Statistical analysis was performed using GraphPad Prism v9.4.0 (GraphPad, USA). Data are represented as mean ± standard deviation (SD). To determine differences between the five groups within the ORX and DGX experiments, a one-way ANOVA followed by Tukey's multiple comparison test was performed. To determine differences between the four groups within the ARKO experiment, a two-way ANOVA followed by Tukey's multiple comparison test was performed. In addition, a one-sample *t*-test was performed on the delta values of body weight and body composition, calculated by subtracting the end point value (day 14) from the baseline value (day 0), to determine whether the change in these parameters throughout the course of the intervention was significantly different from zero. *P*-values <0.05 were considered statistically significant.

## Results

### Validation of androgen deprivation and hormone administration

To determine the effect of endogenous androgen signaling on the metabolic response to glucocorticoids, adult male WT mice were surgically castrated by ORX and compared with control animals (SHAM). Interaction between androgen and glucocorticoid signaling was assessed by supplementing the castrated mice for 2 weeks with VEH, the AR ligand DHT, the GR ligand CORT or a combination of both (CORT + DHT) (Fig. 1A). Changes in the weight of levator ani and bulbocavernosus (LABC) muscle (Rand & Breedlove 1992), seminal vesicles (SV) (Kim *et al.* 2021*b*) and kidney (Khalil *et al.* 2020) confirmed the effectiveness of our hormonal manipulations, as LABC, SV and kidney weights were reduced upon androgen deprivation (ORX + VEH vs SHAM + VEH) and restored by administration of DHT (Fig. 1B, C, D). CORT supplementation alone had no effect on these parameters (Fig. 1B, C, D). Increased glucocorticoid exposure was confirmed by a decrease in adrenal weight upon CORT administration (Spaanderman *et al.* 2018), which was unaltered by castration or DHT supplementation (Fig. 1E). Thymus weight was used as an additional readout for androgen and glucocorticoid action (Viau *et al.* 1999, Li *et al.* 2018, Wilhelmson *et al.* 2018) and was increased after castration and reduced by both DHT and CORT administration (Fig. 1F). Altogether, these observations indicate that the androgen deprivation and the hormonal manipulations with DHT and CORT were effective.

### DHT and CORT differentially modulate body composition

Both androgens and glucocorticoids are known to influence skeletal muscle and fat mass (Spaanderman *et al.* 2018, Li *et al.* 2022). Therefore, we assessed the changes in body composition in our model. Over the 2 weeks of the intervention, the SHAM + VEH mice showed body weight gain, which was absent in

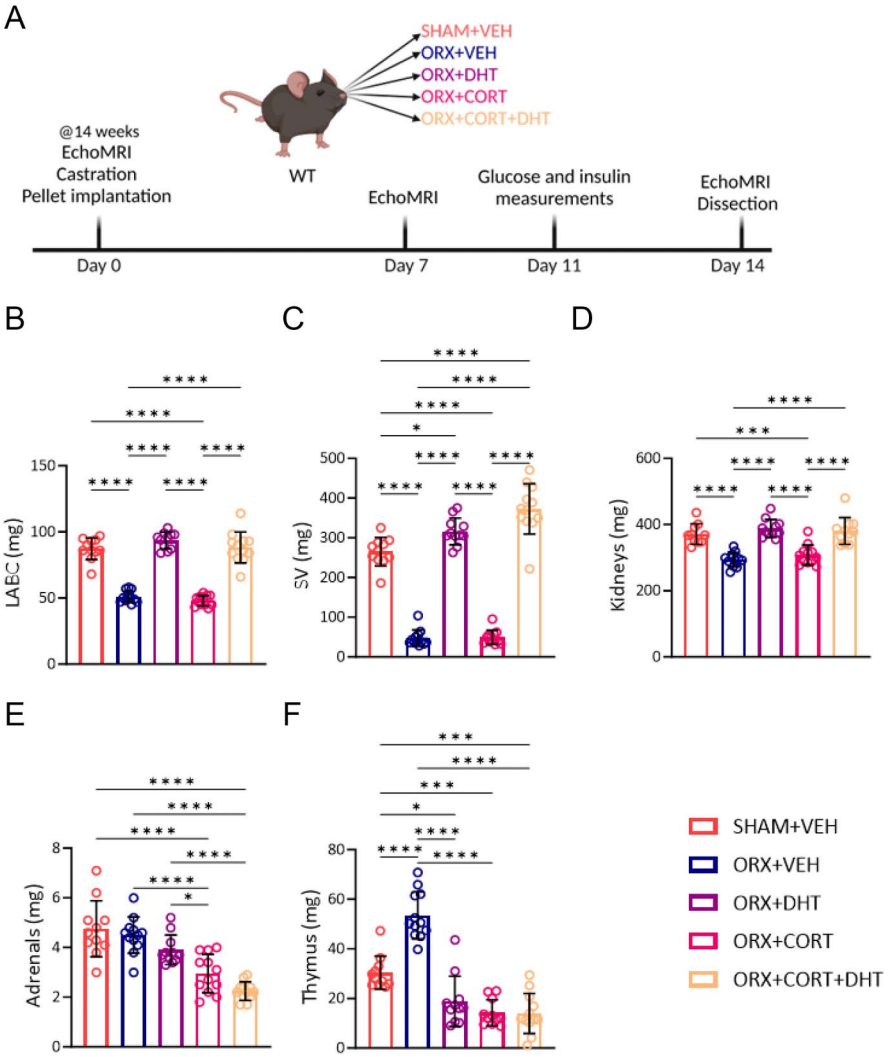


**Figure 1**

Experimental design and validation of androgen deprivation and hormone administration in the ORX model. (A) Fourteen-week-old male WT mice were surgically castrated by orchidectomy (ORX) and supplemented for 2 weeks with vehicle (VEH), dihydrotestosterone (DHT), corticosterone (CORT) or a combination of both (CORT + DHT). The control mice received a SHAM surgery and were supplemented for 2 weeks with VEH. (B, C, D, E and F) Weight (at day 14) of the androgen-sensitive levator ani and bulbocavernosus (LABC) muscle (B), seminal vesicles (SV) (C), kidneys (D), glucocorticoid-sensitive adrenals (E) and glucocorticoid- and androgen-sensitive thymus (F). SHAM + VEH, $n$ = 11; ORX + VEH, $n$ = 12; ORX + DHT, $n$ = 11; ORX + CORT, $n$ = 12; and ORX + CORT + DHT, $n$ = 12. Data are represented as mean ± SD and were analyzed with one-way ANOVA followed by Tukey's multiple comparison test. *$P$ < 0.05, **$P$ < 0.01, ***$P$ < 0.001, ****$P$ < 0.0001. A full colour version of this figure is available at https://doi.org/10.1530/JOE-24-0061.

the ORX + VEH mice but restored by the administration of DHT. Body weight was decreased in the ORX + CORT mice, and this was counteracted by co-administration with DHT (Figs 2A and Supplementary S1A, Supplementary Table S2). These body weight changes were mostly attributable to effects on lean body mass, which was increased by DHT and decreased by CORT. The CORT-induced decrease in lean mass was partially counteracted by co-administration with DHT (Figs 2A and Supplementary S1B, Supplementary Table S2). Gastrocnemius muscle weight decreased in CORT-treated animals (Fig. 2B). The decrease in lean mass in both the ORX + VEH and ORX + CORT animals was accompanied by a decrease in mRNA levels of the *MyHCIIx* gene, a gene encoding for fiber type IIx, which is a fast-twitch glycolytic fiber (Wang & Pessin 2013). Administration of DHT counteracted this decrease in *MyHCIIx* (Fig. 2C). To decipher the molecular pathways involved in the muscle atrophy induced by ORX and CORT, we assessed the expression of the atrogenes *Murf1* and *Mafbx* and of their upstream regulator *Klf15* (Shimizu *et al.* 2011). We observed an unexpected decrease in mRNA levels of *Murf1* and *Mafbx* in ORX + VEH and ORX + CORT compared to SHAM animals (Supplementary Fig. S2A), while *Klf15* expression was unaffected by CORT but decreased in DHT-treated mice (Supplementary Fig. S2B). In line with the phenotypic effects on lean mass, expression of the anabolic marker *Igf-IEa* was decreased upon ORX and increased upon DHT administration (Supplementary Fig. S2C). Altogether, CORT treatment decreased lean mass, which was counteracted by supplementation with DHT. The changes observed in lean mass were paralleled by the changes in mRNA levels of *MyHCIIx*.

We next had a closer look at fat mass, the other main component of body composition next to lean mass. We did not observe major changes in total fat mass in the SHAM + VEH, ORX + VEH and ORX + DHT groups throughout the intervention. In contrast, CORT administration significantly increased fat mass, an effect that was further enhanced in the ORX + CORT + DHT animals (Figs 2A and Supplementary S1C, Supplementary Table S2). In line with this,

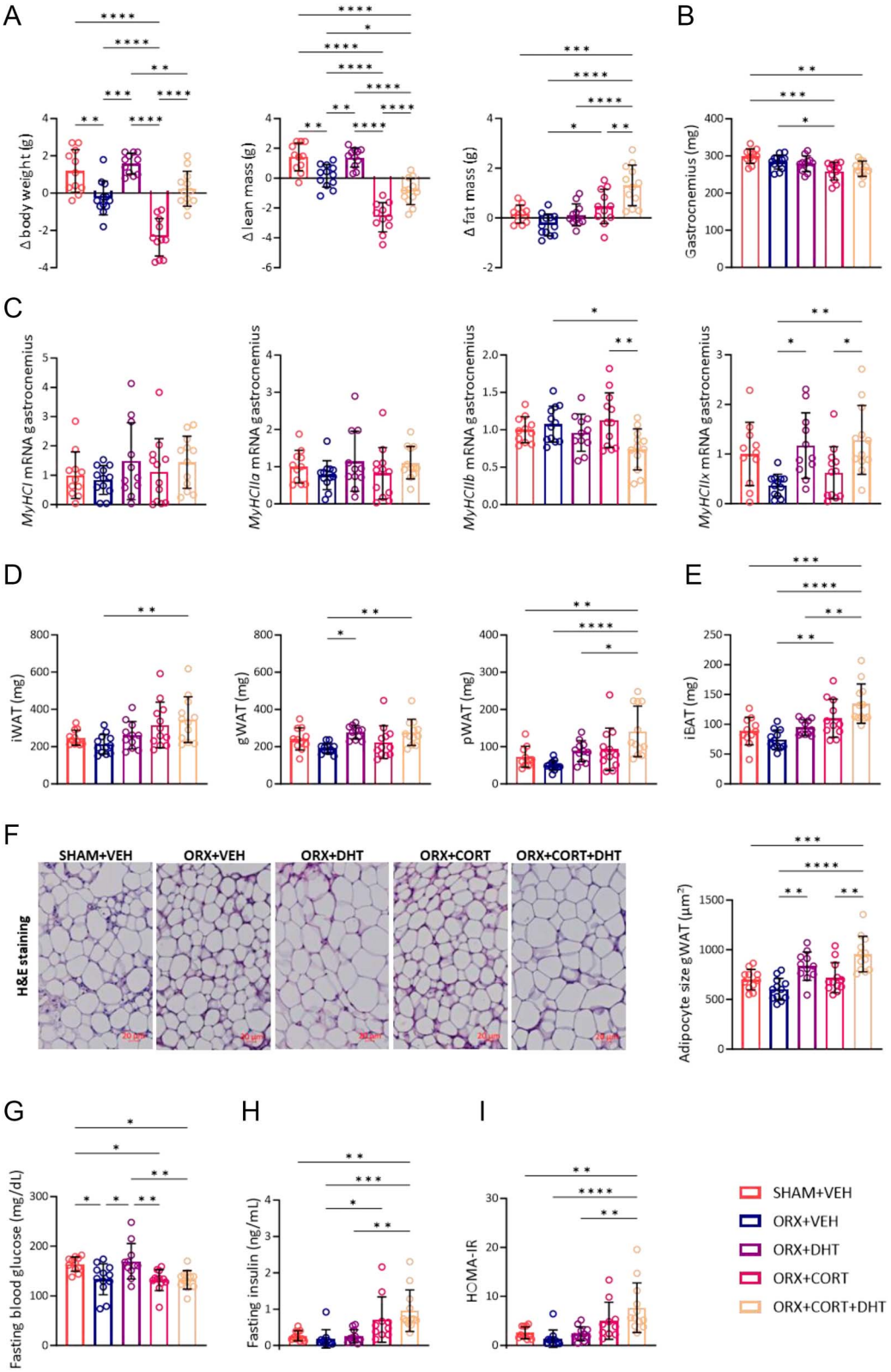


**Figure 2**

Androgen and glucocorticoid effects on body composition and glucose homeostasis in the ORX model. (A) Changes in body weight, lean mass and fat mass (end point day 14 values were subtracted from baseline day 0 values) in SHAM and ORX mice subjected to hormonal manipulations. (B) Weight of the gastrocnemius muscle at day 14. (C) Relative mRNA expression levels of *MyHCI*, *MyHCIIa*, *MyHCIIB* and *MyHCIIx* in gastrocnemius muscle at day 14. (D and E) Weight of inguinal subcutaneous white adipose tissue (iWAT), gonadal white adipose tissue (gWAT), perirenal white adipose tissue (pWAT) (D) and

**Figure 2** (Continued)

interscapular brown adipose tissue (iBAT) (E) fat pads at day 14. (F) Hematoxylin and eosin (H&E) staining of gWAT at day 14. Representative images are displayed along with the mean adipocyte size. Scale bar, 20 μm. (G, H and I) Fasting blood glucose (G), insulin levels (H) and the calculated HOMA-IR (I) at day 11. SHAM + VEH, $n = 11$; ORX + VEH, $n = 12$; ORX + DHT, $n = 11$; ORX + CORT, $n = 12$; ORX + CORT + DHT $n = 12$. Data are represented as mean ± SD and were analyzed with one-way ANOVA followed by Tukey's multiple comparison test. *$P < 0.05$, **$P < 0.01$, ***$P < 0.001$, ****$P < 0.0001$. A full colour version of this figure is available at https://doi.org/10.1530/JOE-24-0061.

the most pronounced increases in the weight of individual fat pads (inguinal, gonadal, perirenal and interscapular) compared to ORX + VEH mice were observed in the ORX + CORT + DHT group (Fig. 2D and E). Furthermore, histological analysis of gWAT revealed an increase in mean adipocyte size in the ORX + DHT and ORX + CORT + DHT animals compared to ORX + VEH animals (Fig. 2F), correlating with the fat pad weight (Fig. 2D). Of note, DHT supplementation alone increased gWAT weight compared to the ORX + VEH group, while CORT on its own augmented interscapular brown adipose tissue (iBAT) weight (Fig. 2D and E). To determine the molecular mechanisms underlying the effects on fat mass, we measured the expression of the lipogenic genes *Pparγ*, *C/EBPα*, *SREBP1c*, *aP2*, *FAS* and *ACC*, and of the lipolytic genes *Lipe* and *Lpl*. The hormonal manipulations had no effect on the expression of any of these genes in gWAT, except for a decrease in *aP2* in ORX + CORT compared to SHAM + VEH animals (Supplementary Fig. S3A). In iBAT, increased expression of *C/EBPα*, *ACC* and *Lipe* was observed in both the ORX + CORT and ORX + CORT + DHT mice (Supplementary Fig. S3B), likely contributing to the increased iBAT weight in these groups (Fig. 2E). Expression of *SREBP1c* was only increased in iBAT from ORX + CORT + DHT animals (Supplementary Fig. S3B). In conclusion, DHT alone did not affect fat mass. In contrast, CORT treatment increased fat mass, an effect that was further enhanced by co-supplementation with DHT.

## Effects of the hormonal manipulations on glucose homeostasis

We assessed glucose homeostasis during the hormonal manipulations, as glucocorticoids regulate glucose metabolism and insulin sensitivity, and this effect might be modulated by androgens (Gasparini *et al.* 2019). Fasting glucose levels were lowered by androgen deprivation (ORX + VEH vs SHAM + VEH) and restored by DHT administration (Fig. 2G). CORT alone had no effect on fasting glucose levels (ORX + CORT vs ORX + VEH) but blunted the restoring effect of DHT (Fig. 2G). Fasting insulin levels were unaffected by androgen deprivation or DHT supplementation but were increased by CORT exposure, suggesting impaired insulin sensitivity in CORT-treated animals (ORX + CORT vs ORX + VEH and ORX + CORT + DHT vs ORX + VEH) (Fig. 2H). These findings are supported by the HOMA-IR, which is an indirect measure of insulin resistance and followed the same pattern as the fasting insulin levels (Fig. 2I). As adipose tissue inflammation is a major driver of insulin resistance (Wu & Ballantyne 2020), we subsequently measured the expression of the pro-inflammatory genes *Il1*, *Il6* and *TNFα* in gWAT. Expression of these cytokines was unaffected by CORT and/or DHT supplementation (Supplementary Fig. S3C). Altogether, CORT treatment increased fasting insulin levels and HOMA-IR. These observations are suggestive of impaired insulin sensitivity in CORT-treated animals, although the involvement of increased pancreatic insulin secretion in these effects cannot be ruled out.

## Effects of the hormonal manipulations on the skeleton

We also evaluated treatment effects on bone mass and architecture, as both androgen (Khalil *et al.* 2020, Kim *et al.* 2021*b*) and glucocorticoid (Canalis & Delany 2002, Hardy *et al.* 2018) signaling influence the skeleton. At the tibial diaphysis, androgen and glucocorticoid effects on cortical bone parameters were marginal, except for a small but significant decrease in total and marrow area in ORX + CORT compared to ORX + VEH animals, confirmed by decreases in endocortical and periosteal perimeters, as well as a slightly lower porosity in this group (Fig. 3A, B, C, D, E, F, G, H). Bone strength was not affected by castration or by androgen and glucocorticoid supplementation, as evidenced by three-point bending analysis (Fig. 3I). At the tibial metaphysis, trabecular bone volume was reduced upon androgen depletion and restored to SHAM levels in the DHT and CORT + DHT mice. In contrast to our expectations, CORT exposure increased trabecular bone volume as compared to ORX + VEH (Fig. 3J). Changes in trabecular bone volume were mostly due to altered trabecular number and concomitant changes in trabecular separation, as trabecular thickness was unaltered except for an increase in the CORT + DHT group (Fig. 3K, L, M). Serum levels of the bone formation marker P1NP were strongly decreased in animals treated with CORT alone, while the circulating levels of the bone resorption marker TRAcP 5b were increased compared to the other experimental conditions. Co-supplementation with DHT in the ORX + CORT + DHT animals restored both markers to SHAM levels (Fig. 3N). Histological analysis of the tibiae mostly mirrored the changes in bone turnover markers, as animals treated with CORT showed a reduction in osteoblast surface and an increase in osteoclast surface. Co-supplementation with DHT prevented the CORT-induced increase in osteoclast surface, which was restored to SHAM levels (Fig. 3O). Altogether, a significant decrease in trabecular bone volume was observed in the ORX + VEH group

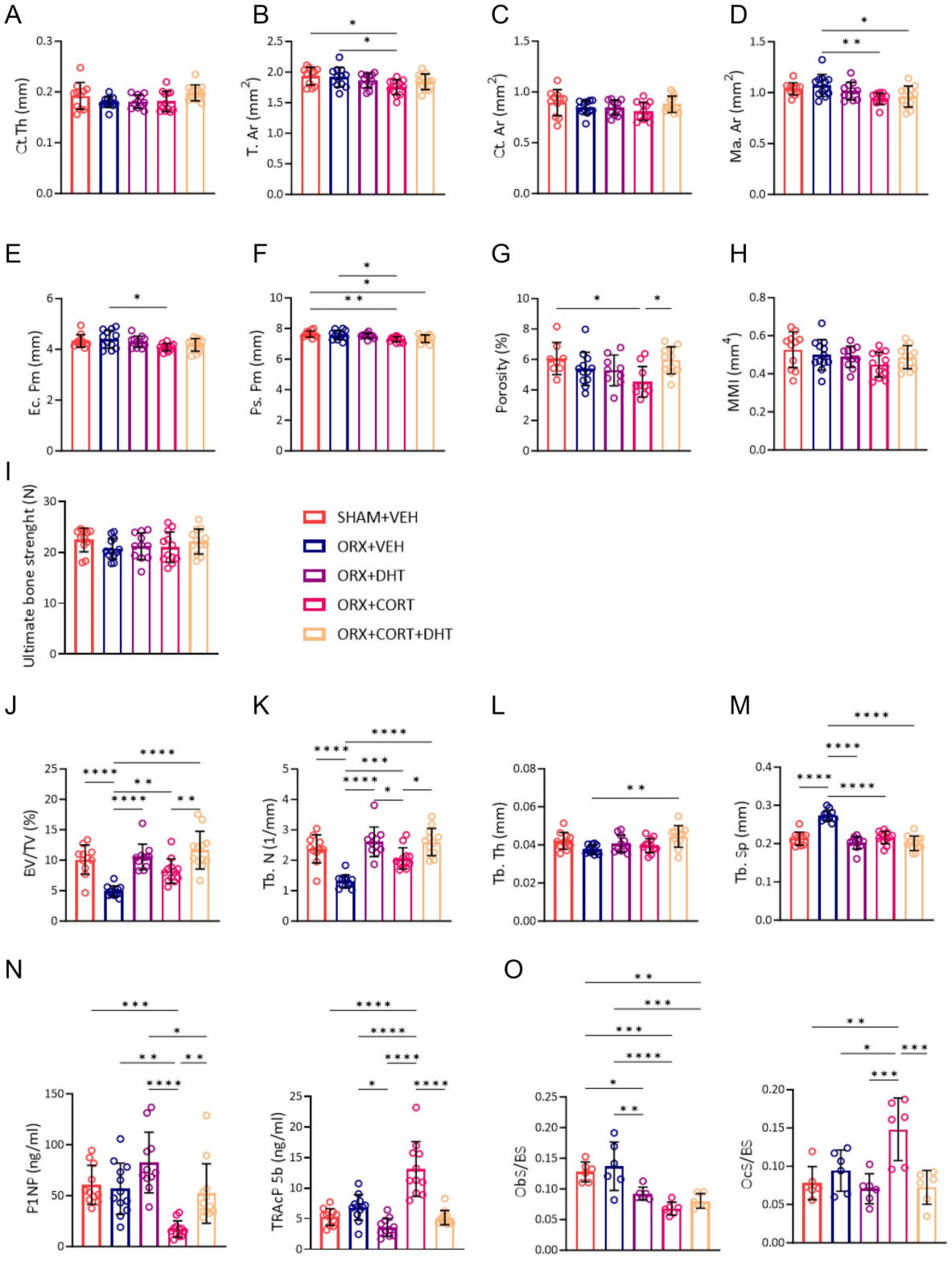


**Figure 3**

Androgen and glucocorticoid effects on bone parameters in the ORX model. (A, B, C, D, E, F, G and H) Effect on cortical bone parameters assessed by microCT at the tibial diaphysis at day 14: cortical thickness (Ct. Th) (A), total tissue area (T. Ar) (B), cortical area (Ct. Ar) (C), medullary area (Ma. Ar) (D), endocortical perimeter (Ec.Pm) (E), periosteal perimeter (Ps. Pm) (F), cortical porosity (G) and polar moment of inertia (MMI) (H). (I) Ultimate bone strength as measured by

**Figure 3** (Continued)

three-point bending. (J, K, L, M) Effect on trabecular bone parameters assessed by microCT at the tibial metaphysis at day 14: trabecular bone volume fraction (BV/TV) (J), trabecular number (Tb. N) (K), trabecular thickness (Tb. Th) (L), trabecular separation (Tb. Sp) (M). (N) Serum concentrations of P1NP and TRAcP 5b at day 14. (O) Quantification of the osteoblast surface per bone surface (Ob.S/BS) and osteoclast surface per bone surface (Oc.S/BS) at the tibial metaphysis at day 14. Sample size in panels A–N: $n$ = 11–12/group. Sample size in panel O: $n$ = 6/group. Data are represented as mean ± SD and were analyzed with one-way ANOVA followed by Tukey's multiple comparison test. *$P$ < 0.05, **$P$ < 0.01, ***$P$ < 0.001, ****$P$ < 0.0001. A full colour version of this figure is available at https://doi.org/10.1530/JOE-24-0061.

compared to the SHAM animals, and this was restored by DHT supplementation. Unexpectedly, ORX animals treated with CORT alone showed an increase in trabecular bone volume compared to ORX + VEH animals, which could not be fully explained by our histological and serum analysis, suggesting that exposure time to glucocorticoids might play a role as bone remodeling is a dynamic process (Kuo & Chen 2017).

## Validation of the DHT and CORT effects in a DGX model

To validate our findings, we used a second model of androgen deprivation, i.e., chemical castration with the GnRH antagonist DGX (Supplementary Fig. S4). DHT and CORT effects were largely similar to those in the ORX model, with lean mass increasing upon DHT treatment in DGX animals but decreasing as a result of CORT administration. Fat mass was not altered by DHT but increased by CORT. Supplementation with CORT furthermore impaired insulin sensitivity, as shown by the increase in fasting insulin levels and HOMA-IR (Supplementary Figs S5 and S6, Supplementary Table S3). In accordance with the ORX model, DGX administration reduced trabecular bone volume due to a reduction in trabecular number and this effect was completely reversed by both DHT and CORT. Cortical bone parameters were unaffected by the hormonal manipulations (Supplementary Fig. S7). Altogether, our observations in two independent models indicate that 2 weeks of DHT administration increases lean mass and trabecular bone volume, while CORT decreases lean mass and increases fat mass and fasting insulin levels in androgen-deprived male WT mice.

## The AR is dispensable for CORT effects on body composition and glucose homeostasis

It has been shown that glucocorticoid treatment upregulates AR in adipose tissue and liver. Furthermore, a study using the AR antagonist enzalutamide indicated that the AR might play a role in the modulation of glucocorticoid effects (Spaanderman *et al.* 2018, Gasparini *et al.* 2019, Buurstede *et al.* 2022). Hence, we next assessed the contribution of the AR in the response to elevated glucocorticoid exposure. Adult male ARKO mice and WT littermates were exposed to either VEH or CORT for 2 weeks (Fig. 4A). Adrenal and thymus weights displayed a two-fold reduction upon CORT administration in both genotypes, indicating that CORT treatment was effective (Fig. 4B and C, Supplementary Table S4). As expected, androgen-sensitive kidney weight was lower in ARKO compared to WT mice, and this was unaffected by CORT administration (Fig. 4D, Supplementary Table S4). The androgen-dependent LABC and SV did not develop in ARKO but were present in WT mice and not influenced by CORT treatment (De Gendt *et al.* 2004, Ipulan *et al.* 2014) (Fig. 4E and F, Supplementary Table S4). CORT treatment decreased body weight in WT animals but not in ARKO mice (Figs 5A and Supplementary S8A, Supplementary Tables S4 and S5). Lean body mass significantly decreased and total fat mass significantly increased upon CORT administration in both genotypes, but the reduction in lean mass was less pronounced in ARKO than in WT animals (Figs 5A, B, Supplementary S8B, C, Supplementary Tables S4 and S5). CORT treatment did not significantly influence the weight of individual fat pads, with the exception of iBAT, which was similarly increased in WT and ARKO mice (Fig. 5C and D, Supplementary Table S4). Fasting glucose levels were similar between the different experimental groups, while fasting insulin levels and HOMA-IR were increased by CORT in both WT and ARKO mice (Fig. 5E and G, Supplementary Table S4). Finally, ARKO mice displayed several skeletal features characteristic of AR deficiency, including markedly reduced trabecular bone volume and number (Supplementary Fig. S9A, B, C, D, Supplementary Table S4) and lower radial bone expansion and cortical thickness (Supplementary Fig. S9E, F, G, H, I, J, K, L, Supplementary Table S4). In both WT and ARKO mice, these parameters were unaffected by the 2 weeks of CORT administration (Supplementary Fig. S9A, B, C, D, E, F, G, H, I, J, K, L, Supplementary Table S4). Altogether, these findings demonstrate that the AR is dispensable for the majority of the effects of elevated CORT on fat mass, lean mass and insulin sensitivity.

## Androgens enhance glucocorticoid-induced transcriptional activity in adipose tissue through the AR

Our observations indicate that a functional AR is not necessary for CORT effects on adiposity (Fig. 5A, C, D), but that administration of the AR ligand DHT does modulate the CORT effects, as evidenced by the higher fat mass gain induced by CORT when co-administered with DHT (Fig. 2A). To further decipher the modulatory effects of androgens on glucocorticoid action in adipose

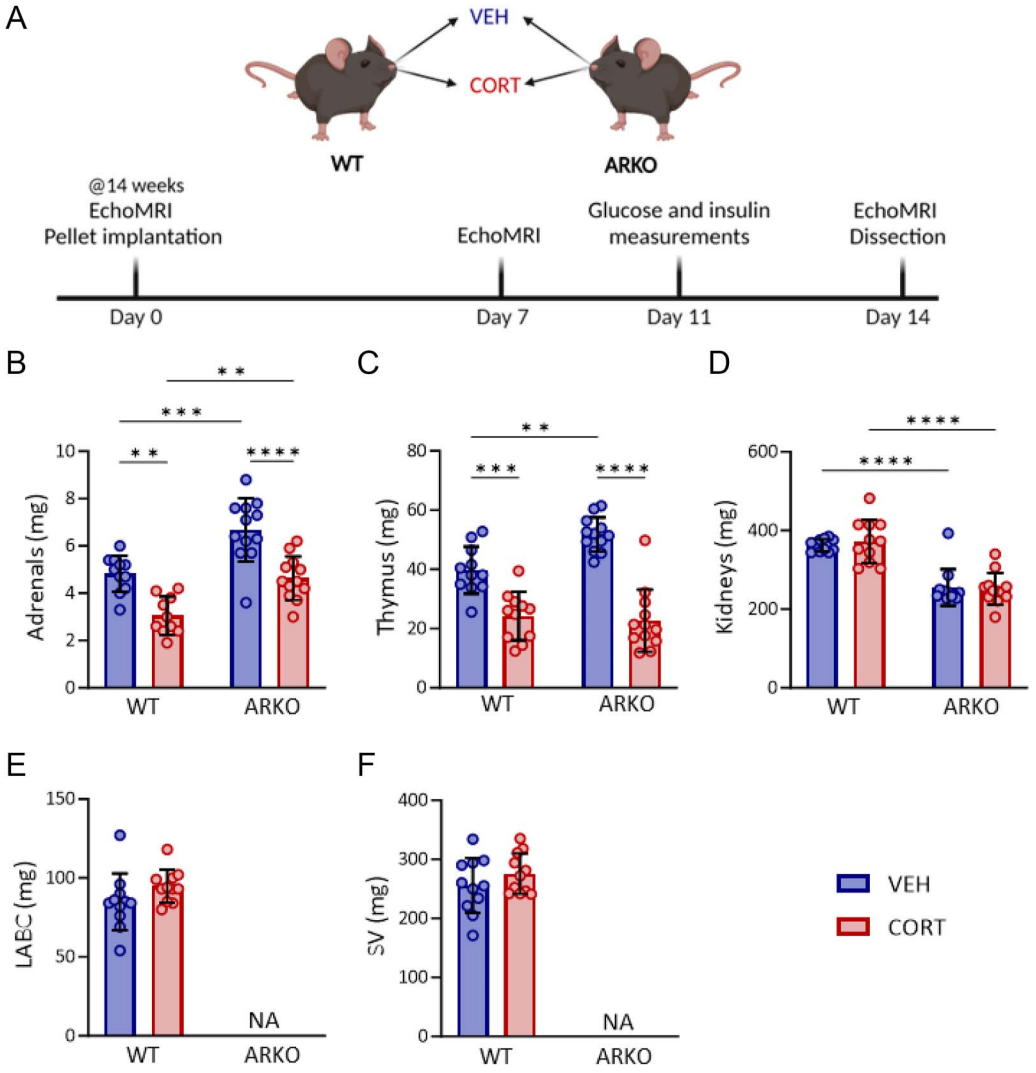


**Figure 4**

Experimental design and validation of glucocorticoid administration in the ARKO model. (A) Fourteen-week-old male ARKO mice and WT littermates were supplemented for 2 weeks with either vehicle (VEH) or corticosterone (CORT). (B, C, D, E and F) Weight (at day 14) of the glucocorticoid-sensitive adrenals (B), the glucocorticoid- and androgen-sensitive thymus (C), the androgen-sensitive kidneys (D), levator ani and bulbocavernosus (LABC) muscle (E) and seminal vesicles (SV) (F). WT + VEH, $n = 11$; WT + CORT, $n = 11$; ARKO + VEH, $n = 12$; and ARKO + CORT, $n = 12$. Data are represented as mean ± SD and were analyzed with two-way ANOVA followed by Tukey's multiple comparison test. $^{**}P < 0.01$, $^{***}P < 0.001$, $^{****}P < 0.0001$. NA, not applicable. A full colour version of this figure is available at https://doi.org/10.1530/JOE-24-0061.

tissue, we evaluated glucocorticoid-regulated transcriptional activity in the different fat pads of the ORX and ARKO models by RT-qPCR analysis of the well-established glucocorticoid-responsive transcripts *Gilz*, *Fkbp5* and *Mt2a* (Wang *et al.* 2019). We focused on the gWAT and iBAT depots, which are highly androgen- and glucocorticoid-responsive, respectively (Van Den Beukel *et al.* 2015, Dubois *et al.* 2016). In the ORX model, gWAT transcript levels of *Gilz* were similar between all experimental groups. Transcript levels of both *Fkbp5* and *Mt2a* were strongly decreased upon androgen deprivation (SHAM + VEH vs ORX + VEH), while DHT supplementation restored expression of these genes. CORT treatment alone had no effect, but co-supplementation with DHT resulted in higher transcript levels in the ORX + DHT + CORT animals compared to all other groups (Fig. 6A). In iBAT, androgen deprivation or DHT supplementation alone did not affect transcript levels of *Gilz*, *Fkbp5* and *Mt2a*. Administration of CORT increased the expression of all three genes, and this was even further increased in the ORX + CORT + DHT mice (Fig. 6B). The enhanced CORT-induced transcriptional activity in gWAT and iBAT upon co-treatment with DHT was not due to increased expression of steroid receptors.

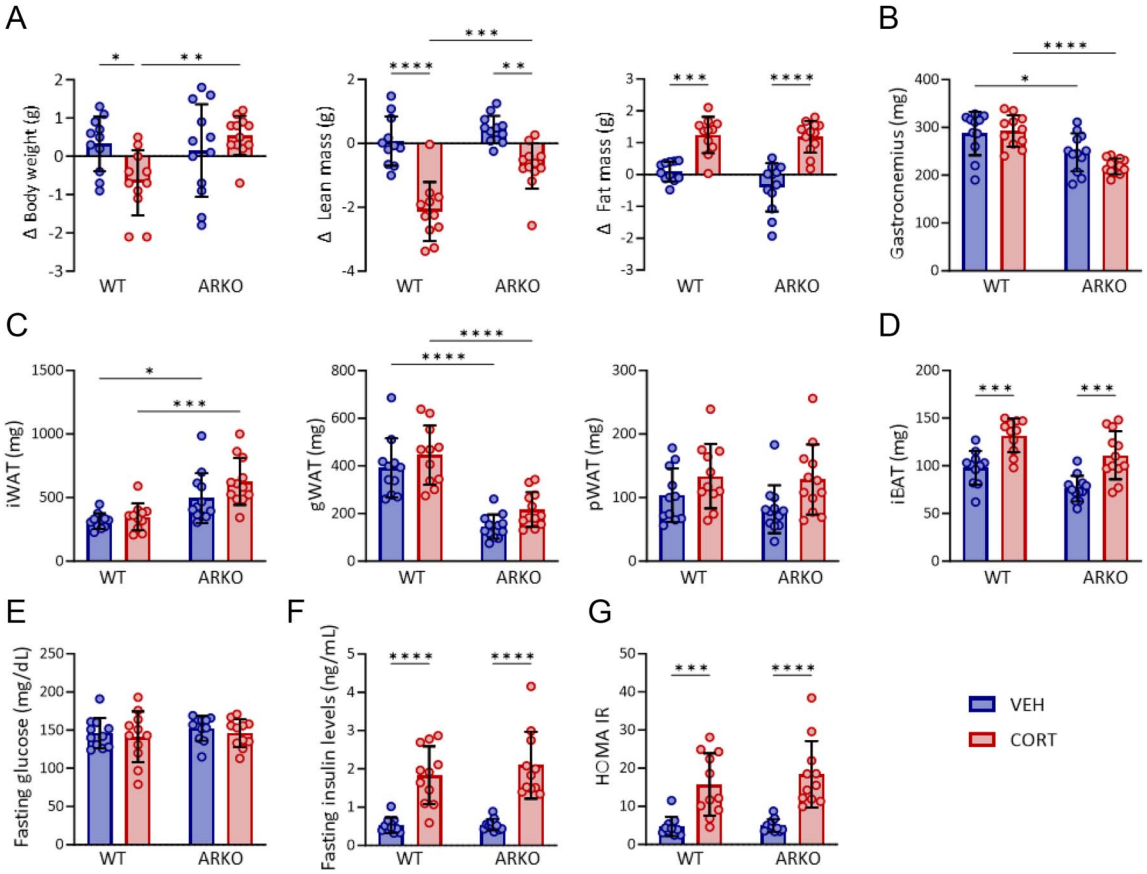


**Figure 5**

Glucocorticoid effects on body composition and glucose homeostasis in the ARKO model. (A) Changes in body weight, lean mass and fat mass (end point day 14 values were subtracted from baseline day 0 values) in WT and ARKO mice exposed to CORT. (B) Weight of the gastrocnemius muscle at day 14. (C, D) Weight of inguinal subcutaneous white adipose tissue (iWAT), gonadal white adipose tissue (gWAT), perirenal white adipose tissue (pWAT) (C) and interscapular brown adipose tissue (iBAT) (D) fat pads at day 14. (E, F, G) Fasting blood glucose (E), insulin levels (F) and the calculated HOMA-IR (G) at day 11. WT + VEH, $n$ = 11; WT + CORT, $n$ = 11; ARKO + VEH, $n$ = 12; and ARKO + CORT, $n$ = 12. Data are represented as mean ± SD and were analyzed with two-way ANOVA followed by Tukey's multiple comparison test. *$P$ < 0.05, **$P$ < 0.01, ***$P$ < 0.001, ****$P$ < 0.0001. A full colour version of this figure is available at https://doi.org/10.1530/JOE-24-0061.

*Ar (Nr3c4)* expression was increased in gWAT and iBAT after CORT exposure, while expression levels of *Gr (Nr3c1)* were similar between all groups. *Mr (Nr3c2)* transcript levels were significantly decreased by ORX in iBAT, with no effects in gWAT (Fig. Supplementary S10A and B).

The ARKO model confirmed the dependence of the CORT induction of *Gilz*, *Fkbp5* and *Mt2a* on AR in gWAT, as the expression of these genes was substantially lower in the VEH-treated ARKO animals compared to their VEH-treated WT counterparts. CORT supplementation increased expression of all three genes in WT but not in ARKO (Fig. 6C, Supplementary Table S4). In iBAT, CORT increased transcript levels of *Gilz*, *Fkbp5* and *Mt2a* both in WT and in ARKO animals, although the response in ARKO was attenuated (Fig. 6D, Supplementary Table S4). In line with our observations in the ORX model, CORT induced *Ar* transcript levels in the iBAT of WT mice, while *Gr* expression was increased by CORT in WT but not ARKO iBAT (Fig. Supplementary S10C and D, Supplementary Table S4). Altogether, our findings suggest that androgens enhance glucocorticoid-induced transcriptional activity in adipose tissue through an AR-dependent mechanism.

To explore whether altered glucocorticoid metabolization might contribute to the modulatory effects of DHT on the response to CORT, we measured transcript levels of the genes encoding the 11β-HSD1 and 11β-HSD2 enzymes, which regulate the balance between active vs inactive glucocorticoids through catalyzation of glucocorticoid activation and inactivation, respectively (Chapman *et al.* 2013, Kadmiel & Cidlowski 2013). We found that *11β-Hsd1* mRNA levels were higher in the gWAT of ORX + CORT + DHT animals compared to ORX animals supplemented with VEH, CORT or DHT alone, while *11β-Hsd2* expression was substantially lower than

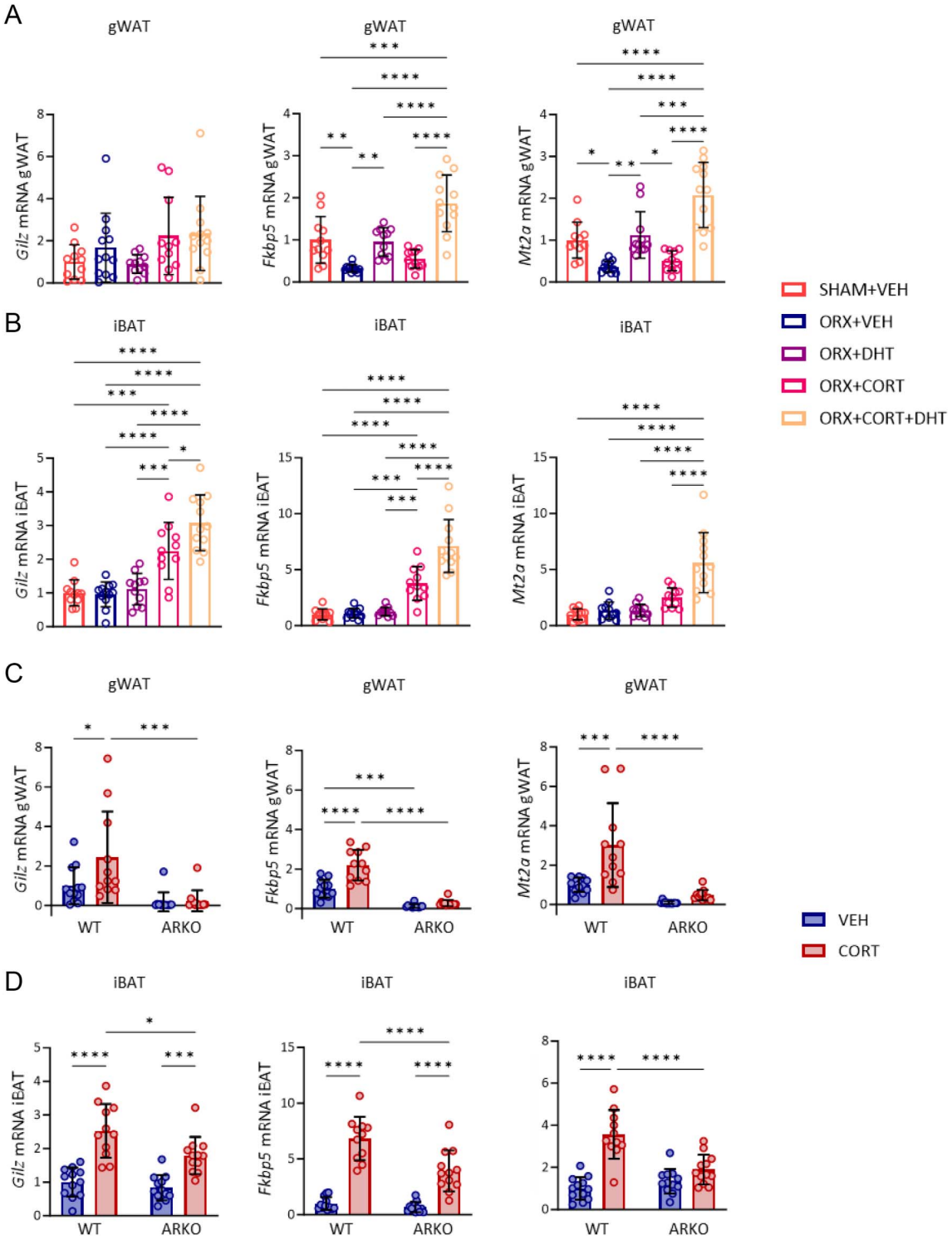


**Figure 6**

Transcript levels of GR-responsive genes in gWAT and iBAT in ORX and ARKO models. (A, B) Relative mRNA expression levels of *Gilz*, *Fkbp5* and *Mt2a* in gWAT (A) and iBAT (B) in the ORX model at day 14. (C, D) Relative mRNA expression levels of *Gilz*, *Fkbp5* and *Mt2a* in gWAT (C) and iBAT (D) in the ARKO model at day 14. SHAM + VEH, $n = 11$; ORX + VEH, $n = 12$; ORX + DHT, $n = 11$; ORX + CORT, $n = 12$; ORX + CORT + DHT, $n = 12$; WT + VEH, $n = 11$; WT + CORT, $n = 11$; ARKO + VEH, $n = 12$; and ARKO + CORT, $n = 12$. Data are represented as mean ± SD and were analyzed with one-way (A, B) or two-way (C, D) ANOVA followed by Tukey's multiple comparison test. *$P < 0.05$, **$P < 0.01$, ***$P < 0.001$, ****$P < 0.0001$. A full colour version of this figure is available at https://doi.org/10.1530/JOE-24-0061.

*Journal of Endocrinology* (2025) **264** e240061
https://doi.org/10.1530/JOE-24-0061

*11b-Hsd1* expression and unaffected by the hormonal manipulations (Fig. 7A). In contrast, in iBAT an increase in *11β-Hsd1* expression was observed in both the ORX + DHT and ORX + CORT groups compared to ORX + VEH but without further increase in the ORX + CORT + DHT animals (Fig. 7B). In the ARKO model, supplementation with CORT increased *11β-Hsd1* expression in gWAT and iBAT in both WT and ARKO animals, while *11β-Hsd2* expression was unaffected (Fig. 7C and D, Supplementary Table S4). In conclusion, we showed differential effects of androgens on gene expression in gWAT and iBAT. In both fat pads, androgens enhance glucocorticoid-induced transcriptional activity. This may be attributed to the increased mRNA expression of *11β-Hsd1*, although further research is needed to confirm changes in enzymatic activity.

## Discussion

In this study, we used two complementary mouse models of androgen deprivation to investigate the role of androgens in the metabolic response to glucocorticoids. Two weeks of DHT supplementation in ORX animals increased lean mass but had no detectable effects on fat mass, while administration of CORT alone decreased lean mass and increased fat mass. We found that androgens are able to influence the effects of glucocorticoids, as co-supplementation with DHT potentiated the effect of CORT on adiposity. To examine the direct contribution of the AR to these effects, CORT action was assessed in the ARKO mouse model. In these mice, we observed that CORT exposure was still able to increase fat mass and decrease lean mass, although the loss of lean mass upon CORT treatment was less pronounced in ARKO compared to WT mice. This suggests that androgen signaling through the AR is mostly dispensable for glucocorticoid effects on body composition but yet is able to modulate CORT effects when present (Fig. 8).

The finding that DHT supplementation alone does not affect fat mass corroborates a previous study from our group in which we showed that androgenic effects on this parameter depend on aromatization into estrogens (Kim *et al.* 2021*a*). It is also in accordance with distinct roles for testosterone and its metabolites DHT and estradiol in the regulation of fat mass and its distribution (Sebo & Rodeheffer 2021). The ability of CORT to increase iBAT weight is in line with a previous study in mice (Doig *et al.* 2017). On the other hand, the observations that CORT increases adiposity and that DHT sensitizes the animals to this effect are supporting the findings of Seibel and colleagues (Gasparini *et al.* 2019), in which androgen presence is shown to be a prerequisite for the metabolic response to CORT. In line with this, we found in iBAT that the induction of GR target genes occurs upon administration of CORT alone and is further enhanced when DHT is co-administered, while in gWAT, a transcriptional response to CORT is only observed in the presence of DHT. The fat depot-specific influence of CORT on gWAT and iBAT was observed not only in the transcriptional response of GR target genes but also in the regulation of lipogenic and lipolytic genes. In our study, CORT treatment did not affect the expression of these genes in gWAT, whereas a CORT response was observed in iBAT for several lipogenic and lipolytic genes. Consistent with these findings, we observed no effect of CORT alone on adipocyte size in gWAT.

CORT increased fat mass in ARKO mice to the same extent as in WT animals, demonstrating that a functional AR is not essential for the increased fat mass observed upon CORT treatment. On the other hand, our observations in the ORX model indicate a modulatory role for androgen signaling on the increased adiposity induced by CORT, as the adipose response to CORT is elevated in the presence of DHT. Our findings do not point toward receptor upregulation as being the main determinant of the enhanced transcriptional activity of CORT upon co-treatment with DHT. It has been previously reported that DHT increases the expression of *11β-Hsd1* mRNA levels in human pre-adipocytes (Dieudonné *et al.* 2006). Interestingly, our findings show a fat depot-specific influence of androgens on the regulation of *11β-Hsd1*, in line with a previous study that compared different human adipose depots (Zhu *et al.* 2010). In our study, *11β-Hsd1* mRNA levels were increased in gWAT of co-supplemented animals compared to mice supplemented with DHT or CORT alone, which might contribute to the magnified transcriptional response in this group, in line with previous findings (Spaanderman *et al.* 2018). It is unclear whether the enzymatic activity of 11β-HSD1 increases along with its transcriptional levels. Next to possible altered glucocorticoid metabolism, gene-specific interplay between androgen and glucocorticoid actions on specific genes or enhancers could take place at the level of direct receptor crosstalk (Chen *et al.* 1997, Sahu *et al.* 2014). For cell-type-specific effects, additional differences in cooperating transcription factors, post-translational modifications or co-regulators might also play a role (Kulik *et al.* 2021).

In both models of androgen deprivation, 2 weeks of supplementation with DHT led to an increased lean body mass, which is in line with the well-established anabolic effects of androgens on skeletal muscle (Dubois *et al.* 2012, Wendowski *et al.* 2017). In contrast, CORT aggravated the ORX- and DGX-associated decrease in lean body mass, which was counteracted by DHT co-administration. In line with these findings, it was previously shown that chemical castration of male mice enhanced the muscle-wasting effects of the synthetic glucocorticoid betamethasone (Li *et al.* 2022). Furthermore, testosterone supplementation in male rats counteracted dexamethasone-induced muscle atrophy (Zhao *et al.* 2008). Rodent skeletal muscle contains four different fiber subtypes, which all have different

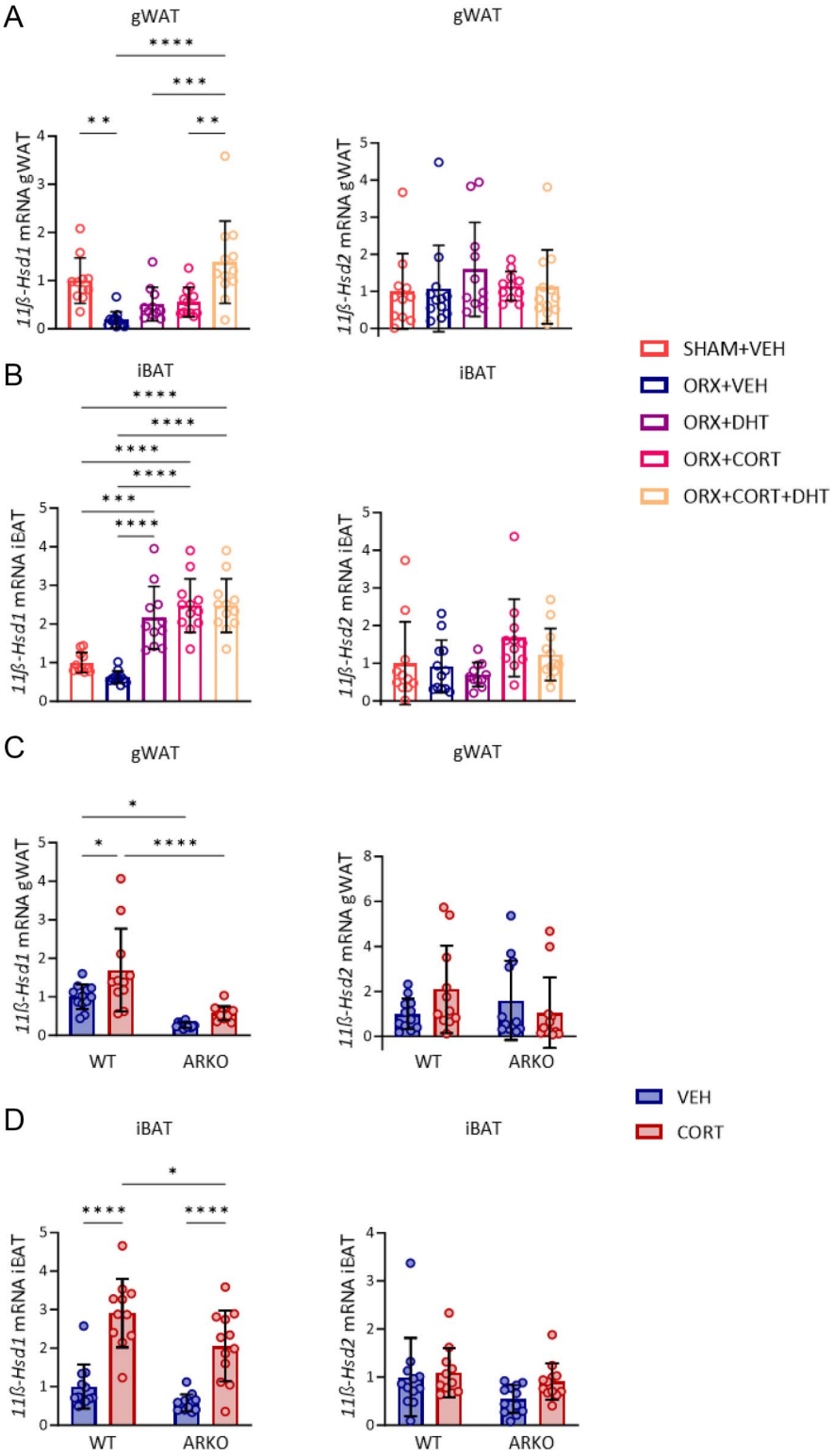


**Figure 7**

Effect of hormone interventions on *11β-Hsd1/2* mRNA levels in the ORX and ARKO models. (A, B) Relative mRNA expression levels of *11β-Hsd1* and *11β-Hsd2* in gWAT (A) and iBAT (B) at day 14 in the ORX model. (C, D) Relative mRNA expression levels of *11β-Hsd1* and *11β-Hsd2* in gWAT (C) and iBAT (D) at day 14 in the ARKO model. SHAM + VEH, $n = 11$; ORX + VEH, $n = 12$; ORX + DHT, $n = 11$; ORX + CORT, $n = 12$; ORX + CORT + DHT, $n = 12$; WT + VEH, $n = 11$ WT + CORT, $n = 11$; ARKO + VEH, $n = 12$; and ARKO + CORT, $n = 12$. Data are represented as mean ± SD and were analyzed with one-way (A, B) or two-way (C, D) ANOVA followed by Tukey's multiple comparison test. $^{*}P < 0.05$, $^{**}P < 0.01$, $^{***}P < 0.001$, $^{****}P < 0.0001$. A full colour version of this figure is available at https://doi.org/10.1530/JOE-24-0061.

sensitivities to muscle degradation. Decreased expression of *MyHCIIx* in gastrocnemius muscle of ORX- and CORT-treated animals supports this notion, as fast-twitch glycolytic fibers are the most sensitive to atrophic environments (Wang & Pessin 2013). The decreased expression of the atrogenes *Murf1* and *Mafbx* upon ORX and CORT exposure is in contrast to the positive regulation of these genes by ORX and CORT reported in the literature (Dubois *et al.* 2012, Bodine & Furlow 2015, Martín *et al.* 2018) and does not point toward the

*Journal of Endocrinology* (2025) **264** e240061
https://doi.org/10.1530/JOE-24-0061

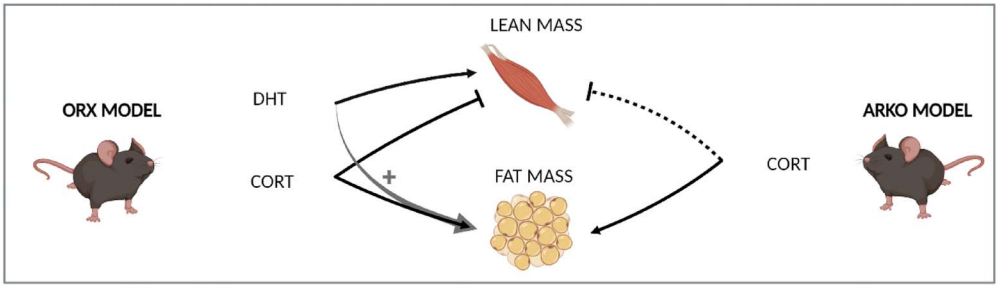


**Figure 8**

Schematic overview of the interplay between androgen and glucocorticoid effects on body composition. In the ORX model of androgen deprivation, DHT increased lean mass and had no detectable effect on fat mass after 2 weeks of treatment. CORT administration, on the other hand, increased fat mass and decreased lean mass. Co-treatment with DHT increased the CORT response on fat mass. The CORT effects on fat and lean mass were also observed in the ARKO model, although the reduction in lean mass was less pronounced in ARKO than in WT animals. Altogether, our findings indicate that androgen signaling through the AR is largely dispensable for glucocorticoid effects on body composition but is able to modulate these effects when present. A full colour version of this figure is available at https://doi.org/10.1530/JOE-24-0061.

involvement of proteasomal degradation in the CORT-induced muscle loss observed in our model. Of note, discrepancies between atrophic effects on muscle mass and expression of atrogenes have been reported previously. As an example, Naeyer and colleagues noted a decrease in the weight of LABC and soleus muscles upon ORX, which was accompanied by increased *Murf1* and *Mafbx* expression in LABC, while in soleus, their expression tended to be decreased (De Naeyer *et al.* 2014). On the other hand, the lower *Igf-IEa* and higher *Klf15* mRNA levels in ORX compared to SHAM animals, with DHT reversing these effects, are in line with the well-known androgen regulation of these genes in skeletal muscle (Dubois *et al.* 2014, 2015). Of note, the reduction in lean mass upon CORT treatment was less pronounced in ARKO compared to WT animals, and we believe that this difference can be attributed to baseline differences in body composition. Specifically (Gomez-Sanchez & Gomez-Sanchez 2014), ARKO animals exhibit a lower proportion of lean mass in comparison with WT animals (Dubois *et al.* 2016), likely rendering them less susceptible to a further reduction in lean mass upon CORT treatment.

In bone, androgen deprivation by both ORX and DGX induced a strong reduction in trabecular bone volume due to a decrease in trabecular number, and this was restored upon DHT supplementation. In contrast, cortical bone was not influenced by castration or DHT supplementation. These findings are in line with the reported higher sensitivity of trabecular bone to circulating androgens (Khalil *et al.* 2020, Kim *et al.* 2021*b*). In neither model of androgen deprivation, we observed the expected CORT-induced bone loss after 2 weeks of CORT administration, although both serum and histological markers of bone formation were decreased by CORT, while those of bone resorption were increased. This discrepancy might be due to the fact that bone remodeling is a dynamic process, and changes in circulating bone turnover markers measured at one specific time point may not always reflect accumulated changes in bone architecture measured with microCT or DEXA (Kuo & Chen 2017). We believe that the lack of visible bone loss in the CORT-treated groups is likely attributable to the relatively short duration of the experimental intervention. Indeed, most of the studies showing detrimental effects of glucocorticoid excess on bone health use a timeframe of 28 days or longer (Wood *et al.* 2018). Accordingly, a synergistic effect on bone loss was shown after 4 weeks of combined ORX and CORT treatment (Badraoui *et al.* 2017). In contrast, another study reported no additional bone loss when combining androgen deprivation with glucocorticoid excess within the same timeframe (Weinstein *et al.* 2004). In our work, 2 weeks of CORT treatment even seemed to have a protective effect on ORX-induced bone loss. We speculate that 2 weeks of CORT treatment might be too short to cause a decrease in bone mass but sufficient to induce a protective anti-inflammatory effect. In line with our hypothesis, treatment with prednisolone reduced inflammation and protected animals from bone erosion after 7 days of treatment in a mouse model of inflammatory arthritis (Perilli *et al.* 2015). Further research is needed to confirm this hypothesis and completely understand the mechanisms underlying the protective effects of short-term glucocorticoid treatment on bone.

Our study has several strengths that contribute to a better understanding of the role of androgen signaling in the metabolic response to glucocorticoids. First, the ORX approach combined with DHT enabled us to assess the exact contribution of androgen signaling through the AR. In contrast to testosterone, DHT cannot be aromatized to estradiol and thus cannot activate the estrogen receptors (Gennari *et al.* 2004). Second, the robustness of our findings was validated using a second model of androgen deprivation, i.e., chemical castration with DGX. Third, we assessed the direct role of the AR in this hormonal interplay by means of the ARKO model. Finally, we studied the interplay between androgens and glucocorticoids in multiple tissues within the same

models. However, our study also has some limitations. Only male animals were studied, which does not enable us to address the impact of androgen status on glucocorticoid effects in females. This is of particular relevance, given the previously reported sexual dimorphic effects of glucocorticoids. Next, the interplay between glucocorticoids and sex steroids might not only include a role for androgens but also for estrogens, which was not addressed in our experimental setting. Of note, while crosstalk with estrogens may still be of relevance for the CORT effects on the musculoskeletal system, the sexually dimorphic effects of glucocorticoids on adipose tissue are likely exclusively due to differences in androgen levels, as ovariectomy did not modulate CORT-induced insulin resistance and fat accumulation (Gasparini *et al.* 2019). It is known that CORT also activates the mineralocorticoid receptor (MR) (Gomez-Sanchez & Gomez-Sanchez 2014) and, therefore, AR-MR crosstalk might contribute to the phenotypic effects in the co-treated animals. Finally, the 2-week timeframe might have been too short to detect hormonal interplay in some tissues, such as the skeleton (Wood *et al.* 2018).

In summary (Fig. 8), we depict that a functional AR is dispensable for the metabolic response to glucocorticoids. When present, intact androgen signaling modulates the glucocorticoid response by counteracting the effects on lean mass and potentiating the effects on fat mass.

**Supplementary materials**

This is linked to the online version of the paper at https://doi.org/10.1530/JOE-24-0061.

**Declaration of interest**

OCM receives research funding from Corcept Therapeutics. JK is seconded to Corcept Therapeutics for 50% of his time. Other authors have nothing to disclose.

**Funding**

This work was funded by a KU Leuven grant (C14/19/100). VS is a recipient of a Global PhD partnership between LUMC and KU Leuven.

**Author contribution statement**

VS, CH, SS, RD, JK, OCM, FC and VD conceptualized the study. VS, KD, KM, IS, GF and VD performed the experimental work. VS analyzed the data. VS wrote the first draft of the manuscript with assistance from VD, FC, JK and OCM. All authors reviewed and edited the manuscript before submission.

**Acknowledgements**

The authors thank Ludo Deboel, Dieter Schollaert, Annelies Smit and Reshma Lalai for their technical support and Dirk Vanderschueren, Brigitte Decallonne, Leen Antonio and Nick Narinx for the fruitful discussions.

## References

Arora VK, Schenkein E, Murali R, *et al.* 2013 Glucocorticoid receptor confers resistance to antiandrogens by bypassing androgen receptor blockade. *Cell* **155** 1309–1322. (https://doi.org/10.1016/j.cell.2013.11.012)

Badraoui R, Amri N, Zammel N, *et al.* 2017 Corticosteroid treatment exacerbates bone osteopenia in mice with gonadal hormone deficiency-induced osteoporosis. *Eur J Pharm Sci* **105** 41–46. (https://doi.org/10.1016/j.ejps.2017.04.023)

Bodine SC & Furlow JD 2015 Glucocorticoids and skeletal muscle. *Adv Exp Med Biol* **872** 145–176. (https://doi.org/10.1007/978-1-4939-2895-8_7)

Buurstede JC, Paul SN, De Bosscher K, *et al.* 2022 Hepatic glucocorticoid-induced transcriptional regulation is androgen-dependent after chronic but not acute glucocorticoid exposure. *FASEB J* **36** e22251. (https://doi.org/10.1096/fj.202101313r)

Canalis E & Delany AM 2002 Mechanisms of glucocorticoid action in bone. *Ann N Y Acad Sci* **966** 73–81. (https://doi.org/10.1111/j.1749-6632.2002.tb04204.x)

Chapman K, Holmes M & Seckl J 2013 11β-Hydroxysteroid dehydrogenases: intracellular gate-keepers of tissue glucocorticoid action. *Physiol Rev* **93** 1139–1206. (https://doi.org/10.1152/physrev.00020.2012)

Chen S, Wang J, Yu G, *et al.* 1997 Androgen and glucocorticoid receptor heterodimer formation. *J Biol Chem* **272** 14087–14092. (https://doi.org/10.1074/jbc.272.22.14087)

Coutinho AE, Gray M, Brownstein DG, *et al.* 2012 11β-Hydroxysteroid dehydrogenase type 1, but not type 2, deficiency worsens acute inflammation and experimental arthritis in mice. *Endocrinology* **153** 234–240. (https://doi.org/10.1210/en.2011-1398)

Davies P & Rushmere NK 1990 Association of glucocorticoid receptors with prostate nuclear sites for androgen receptors and with androgen response elements. *J Mol Endocrinol* **5** 117–127. (https://doi.org/10.1677/jme.0.0050117)

De Bosscher K, Desmet SJ, Clarisse D, *et al.* 2020 Nuclear receptor crosstalk - defining the mechanisms for therapeutic innovation. *Nat Rev Endocrinol* **16** 363–377. (https://doi.org/10.1038/s41574-020-0349-5)

De Gendt K, Swinnen JV, Saunders PT, *et al.* 2004 A Sertoli cell-selective knockout of the androgen receptor causes spermatogenic arrest in meiosis. *Proc Natl Acad Sci U S A* **101** 1327–1332. (https://doi.org/10.1073/pnas.0308114100)

De Naeyer H, Lamon S, Russell AP, *et al.* 2014 Androgenic and estrogenic regulation of Atrogin-1, MuRF1 and myostatin expression in different muscle types of male mice. *Eur J Appl Physiol* **114** 751–761. (https://doi.org/10.1007/s00421-013-2800-y)

Dempster DW, Compston JE, Drezner MK, *et al.* 2013 Standardized nomenclature, symbols, and units for bone histomorphometry: a 2012 update of the report of the ASBMR Histomorphometry Nomenclature Committee. *J Bone Miner Res* **28** 2–17. (https://doi.org/10.1002/jbmr.1805)

Dieudonné MN, Sammari A, Dos Santos E, *et al.* 2006 Sex steroids and leptin regulate 11β-hydroxysteroid dehydrogenase I and P450 aromatase expressions in human preadipocytes: sex specificities. *J Steroid Biochem Mol Biol* **99** 189–196. (https://doi.org/10.1016/j.jsbmb.2006.01.007)

Doig CL, Fletcher RS, Morgan SA, *et al.* 2017 11β-HSD1 modulates the set point of brown adipose tissue response to glucocorticoids in male mice. *Endocrinology* **158** 1964–1976. (https://doi.org/10.1210/en.2016-1722)

Dubois V, Laurent M, Boonen S, *et al.* 2012 Androgens and skeletal muscle: cellular and molecular action mechanisms underlying the anabolic actions. *Cell Mol Life Sci* **69** 1651–1667. (https://doi.org/10.1007/s00018-011-0883-3)

Dubois V, Laurent MR, Sinnesael M, *et al.* 2014 A satellite cell-specific knockout of the androgen receptor reveals myostatin as a direct androgen target in skeletal muscle. *FASEB J* **28** 2979–2994. (https://doi.org/10.1096/fj.14-249748)

Dubois V, Simitsidellis I, Laurent MR, *et al.* 2015 Enobosarm (GTx-024) modulates adult skeletal muscle mass independently of the androgen receptor in the satellite cell lineage. *Endocrinology* **156** 4522–4533. (https://doi.org/10.1210/en.2015-1479)

Dubois V, Laurent MR, Jardi F, *et al.* 2016 Androgen deficiency exacerbates high-fat diet-induced metabolic alterations in male mice. *Endocrinology* **157** 648–665. (https://doi.org/10.1210/en.2015-1713)

Duma D, Collins JB, Chou JW, *et al.* 2010 Sexually dimorphic actions of glucocorticoids provide a link to inflammatory diseases with gender differences in prevalence. *Sci Signal* **3** ra74. (https://doi.org/10.1126/scisignal.2001077)

Gasparini SJ, Swarbrick MM, Kim S, *et al.* 2019 Androgens sensitise mice to glucocorticoid-induced insulin resistance and fat accumulation. *Diabetologia* **62** 1463–1477. (https://doi.org/10.1007/s00125-019-4887-0)

Gennari L, Nuti R & Bilezikian JP 2004 Aromatase activity and bone homeostasis in men. *J Clin Endocrinol Metab* **89** 5898–5907. (https://doi.org/10.1210/jc.2004-1717)

Gomez-Sanchez E & Gomez-Sanchez CE 2014 The multifaceted mineralocorticoid receptor. *Compr Physiol* **4** 965–994. (https://doi.org/10.1002/cphy.c130044)

Hardy RS, Zhou H, Seibel MJ, *et al.* 2018 Glucocorticoids and bone: consequences of endogenous and exogenous excess and replacement therapy. *Endocr Rev* **39** 519–548. (https://doi.org/10.1210/er.2018-00097)

Hua C, Buttgereit F & Combe B 2020 Glucocorticoids in rheumatoid arthritis: current status and future studies. *RMD Open* **6** e000536. (https://doi.org/10.1136/rmdopen-2017-000536)

Huan C, Qu Y & Ren Z 2014 Gender differences in presentation and outcome of patients with Cushing's disease in Han Chinese. *Biomed Mater Eng* **24** 3439–3446. (https://doi.org/10.3233/bme-141168)

Ipulan LA, Suzuki K, Sakamoto Y, *et al.* 2014 Nonmyocytic androgen receptor regulates the sexually dimorphic development of the embryonic bulbocavernosus muscle. *Endocrinology* **155** 2467–2479. (https://doi.org/10.1210/en.2014-1008)

Kadmiel M & Cidlowski JA 2013 Glucocorticoid receptor signaling in health and disease. *Trends Pharmacol Sci* **34** 518–530. (https://doi.org/10.1016/j.tips.2013.07.003)

Kaikaew K, Steenbergen J, Van Dijk TH, *et al.* 2019 Sex difference in corticosterone-induced insulin resistance in mice. *Endocrinology* **160** 2367–2387. (https://doi.org/10.1210/en.2019-00194)

Khalil R, Simitsidellis I, Kim NR, *et al.* 2020 Androgen action on renal calcium and phosphate handling: effects of bisphosphonate treatment and low calcium diet. *Mol Cell Endocrinol* **514** 110891. (https://doi.org/10.1016/j.mce.2020.110891)

Kim NR, Jardí F, Khalil R, *et al.* 2020 Estrogen receptor alpha signaling in extrahypothalamic neurons during late puberty decreases bone size and strength in female but not in male mice. *FASEB J* **34** 7118–7126. (https://doi.org/10.1096/fj.202000272r)

Kim NR, David K, Corbeels K, *et al.* 2021*a* Testosterone reduces body fat in male mice by stimulation of physical activity via extrahypothalamic ERα signaling. *Endocrinology* **162** bqab045. (https://doi.org/10.1210/endocr/bqab045)

Kim NR, Khalil R, David K, *et al.* 2021*b* Novel model to study the physiological effects of temporary or prolonged sex steroid deficiency in male mice. *Am J Physiol Endocrinol Metab* **320** E415–e424. (https://doi.org/10.1152/ajpendo.00401.2020)

Koorneef LL, Kroon J, Viho EMG, *et al.* 2020 The selective glucocorticoid receptor antagonist CORT125281 has tissue-specific activity. *J Endocrinol* **246** 79–92. (https://doi.org/10.1530/joe-19-0486)

Kroon J, Pereira AM & Meijer OC 2020 Glucocorticoid sexual dimorphism in metabolism: dissecting the role of sex hormones. *Trends Endocrinol Metab* **31** 357–367. (https://doi.org/10.1016/j.tem.2020.01.010)

Kulik M, Bothe M, Kibar G, *et al.* 2021 Androgen and glucocorticoid receptor direct distinct transcriptional programs by receptor-specific and shared DNA binding sites. *Nucleic Acids Res* **49** 3856–3875. (https://doi.org/10.1093/nar/gkab185)

Kuo T-R & Chen C-H 2017 Bone biomarker for the clinical assessment of osteoporosis: recent developments and future perspectives. *Biomark Res* **5** 18. (https://doi.org/10.1186/s40364-017-0097-4)

Li T, Yan F, Meng X, *et al.* 2018 Improvement of glucocorticoid-impaired thymus function by dihydromyricetin via up-regulation of PPARγ-associated fatty acid metabolism. *Pharmacol Res* **137** 76–88. (https://doi.org/10.1016/j.phrs.2018.09.011)

Li S, Schönke M, Buurstede JC, *et al.* 2022 Sexual dimorphism in transcriptional and functional glucocorticoid effects on mouse skeletal muscle. *Front Endocrinol* **13** 907908. (https://doi.org/10.3389/fendo.2022.907908)

Martín AI, Priego T & López-Calderón A 2018 Hormones and muscle atrophy. *Adv Exp Med Biol* **1088** 207–233. (https://doi.org/10.1007/978-981-13-1435-3_9)

Okita K, Iwahashi H, Kozawa J, *et al.* 2013 Homeostasis model assessment of insulin resistance for evaluating insulin sensitivity in patients with type 2 diabetes on insulin therapy. *Endocr J* **60** 283–290. (https://doi.org/10.1507/endocrj.ej12-0320)

Paakinaho V & Palvimo JJ 2021 Genome-wide crosstalk between steroid receptors in breast and prostate cancers. *Endocr Relat Cancer* **28** R231–R250. (https://doi.org/10.1530/erc-21-0038)

Pecori Giraldi F, Moro M & Cavagnini F 2003 Gender-related differences in the presentation and course of Cushing's disease. *J Clin Endocrinol Metab* **88** 1554–1558. (https://doi.org/10.1210/jc.2002-021518)

Perilli E, Cantley M, Marino V, *et al.* 2015 Quantifying not only bone loss, but also soft tissue swelling, in a murine inflammatory arthritis model using micro-computed tomography. *Scand J Immunol* **81** 142–150. (https://doi.org/10.1111/sji.12259)

Poetker DM & Reh DD 2010 A comprehensive review of the adverse effects of systemic corticosteroids. *Otolaryngol Clin North Am* **43** 753–768. (https://doi.org/10.1016/j.otc.2010.04.003)

Præstholm SM, Correia CM & Grøntved L 2020 Multifaceted control of GR signaling and its impact on hepatic transcriptional networks and metabolism. *Front Endocrinol* **11** 572981. (https://doi.org/10.3389/fendo.2020.572981)

Quinn M, Ramamoorthy S & Cidlowski JA 2014 Sexually dimorphic actions of glucocorticoids: beyond chromosomes and sex hormones. *Ann N Y Acad Sci* **1317** 1–6. (https://doi.org/10.1111/nyas.12425)

Rand MN & Breedlove SM 1992 Androgen locally regulates rat bulbocavernosus and levator ani size. *J Neurobiol* **23** 17–30. (https://doi.org/10.1002/neu.480230104)

Sahu B, Laakso M, Pihlajamaa P, *et al.* 2013 FoxA1 specifies unique androgen and glucocorticoid receptor binding events in prostate cancer cells. *Cancer Res* **73** 1570–1580. (https://doi.org/10.1158/0008-5472.can-12-2350)

Sahu B, Pihlajamaa P, Dubois V, *et al.* 2014 Androgen receptor uses relaxed response element stringency for selective chromatin binding and transcriptional regulation in vivo. *Nucleic Acids Res* **42** 4230–4240. (https://doi.org/10.1093/nar/gkt1401)

Savas M, Muka T, Wester VL, *et al.* 2017 Associations between systemic and local corticosteroid use with metabolic syndrome and body mass index. *J Clin Endocrinol Metab* **102** 3765–3774. (https://doi.org/10.1210/jc.2017-01133)

Sebo ZL & Rodeheffer MS 2021 Testosterone metabolites differentially regulate obesogenesis and fat distribution. *Mol Metab* **44** 101141. (https://doi.org/10.1016/j.molmet.2020.101141)

Shimizu N, Yoshikawa N, Ito N, *et al.* 2011 Crosstalk between glucocorticoid receptor and nutritional sensor mTOR in skeletal muscle. *Cell Metab* **13** 170–182. (https://doi.org/10.1016/j.cmet.2011.01.001)

Spaanderman DCE, Nixon M, Buurstede JC, *et al.* 2018 Androgens modulate glucocorticoid receptor activity in adipose tissue and liver. *J Endocrinol* **240** 51–63. (https://doi.org/10.1530/JOE-18-0503)

Stegen S, Moermans K, Stockmans I, *et al.* 2024 The serine synthesis pathway drives osteoclast differentiation through epigenetic regulation of NFATc1 expression. *Nat Metab* **6** 141–152. (https://doi.org/10.1038/s42255-023-00948-y)

Valassi E, Santos A, Yaneva M, *et al.* 2011 The European Registry on Cushing's syndrome: 2-year experience. Baseline demographic and clinical characteristics. *Eur J Endocrinol* **165** 383–392. (https://doi.org/10.1530/eje-11-0272)

Van Den Beukel JC, Boon MR, Steenbergen J, *et al.* 2015 Cold exposure partially corrects disturbances in lipid metabolism in a male mouse model of glucocorticoid excess. *Endocrinology* **156** 4115–4128. (https://doi.org/10.1210/en.2015-1092)

Vandenput L, Boonen S, Van Herck E, *et al.* 2002 Evidence from the aged orchidectomized male rat model that 17β-estradiol is a more effective bone-sparing and anabolic agent than 5α-dihydrotestosterone. *J Bone Miner Res* **17** 2080–2086. (https://doi.org/10.1359/jbmr.2002.17.11.2080)

Vandevyver S, Dejager L & Libert C 2014 Comprehensive overview of the structure and regulation of the glucocorticoid receptor. *Endocr Rev* **35** 671–693. (https://doi.org/10.1210/er.2014-1010)

Viau V, Chu A, Soriano L, *et al.* 1999 Independent and overlapping effects of corticosterone and testosterone on corticotropin-releasing hormone and arginine vasopressin mRNA expression in the paraventricular nucleus of the hypothalamus and stress-induced adrenocorticotropic hormone release. *J Neurosci* **19** 6684–6693. (https://doi.org/10.1523/jneurosci.19-15-06684.1999)

Walker BR & Andrew R 2006 Tissue production of cortisol by 11β-hydroxysteroid dehydrogenase type 1 and metabolic disease. *Ann N Y Acad Sci* **1083** 165–184. (https://doi.org/10.1196/annals.1367.012)

Wang Y & Pessin JE 2013 Mechanisms for fiber-type specificity of skeletal muscle atrophy. *Curr Opin Clin Nutr Metab Care* **16** 243–250. (https://doi.org/10.1097/mco.0b013e328360272d)

Wang C, Nanni L, Novakovic B, *et al.* 2019 Extensive epigenomic integration of the glucocorticoid response in primary human monocytes and in vitro derived macrophages. *Sci Rep* **9** 2772. (https://doi.org/10.1038/s41598-019-39395-9)

Weinstein RS, Jia D, Powers CC, *et al.* 2004 The skeletal effects of glucocorticoid excess override those of orchidectomy in mice. *Endocrinology* **145** 1980–1987. (https://doi.org/10.1210/en.2003-1133)

Wendowski O, Redshaw Z & Mutungi G 2017 Dihydrotestosterone treatment rescues the decline in protein synthesis as a result of sarcopenia in isolated mouse skeletal muscle fibres. *J Cachexia Sarcopenia Muscle* **8** 48–56. (https://doi.org/10.1002/jcsm.12122)

Whittier DE, Boyd SK, Burghardt AJ, *et al.* 2020 Guidelines for the assessment of bone density and microarchitecture in vivo using high-resolution peripheral quantitative computed tomography. *Osteoporos Int* **31** 1607–1627. (https://doi.org/10.1007/s00198-020-05438-5)

Wilhelmson AS, Lantero Rodriguez M, Svedlund Eriksson E, *et al.* 2018 Testosterone protects against atherosclerosis in male mice by targeting thymic epithelial cells-brief report. *Arterioscler Thromb Vasc Biol* **38** 1519–1527. (https://doi.org/10.1161/atvbaha.118.311252)

Wood CL, Soucek O, Wong SC, *et al.* 2018 Animal models to explore the effects of glucocorticoids on skeletal growth and structure. *J Endocrinol* **236** R69–r91. (https://doi.org/10.1530/joe-17-0361)

Wu H & Ballantyne CM 2020 Metabolic inflammation and insulin resistance in obesity. *Circ Res* **126** 1549–1564. (https://doi.org/10.1161/circresaha.119.315896)

Zhao W, Pan J, Zhao Z, *et al.* 2008 Testosterone protects against dexamethasone-induced muscle atrophy, protein degradation and MAFbx upregulation. *J Steroid Biochem Mol Biol* **110** 125–129. (https://doi.org/10.1016/j.jsbmb.2008.03.024)

Zhu L, Hou M, Sun B, *et al.* 2010 Testosterone stimulates adipose tissue 11β-hydroxysteroid dehydrogenase type 1 expression in a depot-specific manner in children. *J Clin Endocrinol Metab* **95** 3300–3308. (https://doi.org/10.1210/jc.2009-2708)